[SSC21-V-03]

Optimal Attitude Guidance for the EXACT and IMPRESS CubeSats using Graph Methods with Pruning

Athanasios Pantazides, Demoz Gebre-Egziabher
University of Minnesota
110 Union St. SE Minneapolis, MN 55455
panta013@umn.edu

ABSTRACT

This work demonstrates a high-level mission planning method for maximizing data output from a pair of scientific CubeSat missions. The proposed approach identifies the optimal sequence of attitude maneuvers to perform in order to maximize total downlinked data over the mission, while considering constraints on available power. Many scientific satellite missions consist of at least three target attitudes: pointing solar panels towards the Sun for power, pointing an antenna towards a groundstation to transmit data, or pointing a payload towards a point of scientific interest. While careful mechanical design of the mission may enable all three (or more) target attitudes to be achieved simultaneously in certain cases, in general a decision must be made about which target to point to at what time in order to optimally achieve mission objectives and satisfy mission constraints. In this work, we develop a mission planning method that maximizes the volume of data downlinked to the ground over the mission time horizon while respecting constraints on battery level. The optimization problem is posed as an integer program over the space of attitude trajectories and subject to battery constraints. The solution of this problem is an attitude sequence that can be used as a reference for a low-level attitude controller to track. Previous work on this problem suffered from slow solution time for complex mission scenarios which constrained the realism of simulations performed for validation, so in this work we build on our prior approach by leveraging more advanced pruning and search methods to improve optimizer efficiency. We demonstrate the proposed approach on two CubeSats: IMPRESS and EXACT, both currently in design and sharing many mechanical specifications. Both CubeSats are controlled by low-bandwidth actuators and have three main attitude targets: the Sun for power, the Crab Nebula or the Sun the scientific mission, and ground stations for communication. Using simulated orbit data, we show the effectiveness of this method in squeezing mission performance out of both CubeSats while maintaining on-board power. Additionally, the proposed method can run faster than real-time for time horizons of several orbits, enabling a high level of autonomy in orbit.

Introduction

CubeSats are a class of nano-satellites which are constructed from modular 10 cm × 10 cm × 10 cm cubic units known as "U." CubeSats are attractive platforms for scientific research because they can be easily and inexpensively built by an organization whose primary mission is not building aerospace vehicles. This has been enabled, in part, by the availability of off-the-shelf sensors, systems and software that can be used to assemble these miniature spacecraft rapidly and inexpensively. However, the power constraints on CubeSats are severe because the amount of surface area for solar cells on CubeSats is limited. Because of cost and power constraints, many small CubeSats use inexpensive but low bandwidth attitude control systems. The power and control constraints necessitates that care be taken when planning missions for CubeSats. Poor mission planning, for example, can result in a CubeSat draining its batteries before it can maneuver into a position favorable for charging them using solar panels. This paper deals with the mission planning problem for a pair of 3U CubeSats, taking into account the severe power constraints.

The IMpulsive Phase Rapid Energetic Solar Spectrometer (IMPRESS) is a 3U CubeSat mission that will fly a compact x-ray spectrometer to perform soft and hard x-ray (SXR and HXR, respectively) spectroscopy of solar flares in the rising phase of Solar Cycle 25.[1] IMPRESS is optimized to observe high-cadence HXR and SXR spectra from a wide range of solar flares (targeting C1 to X1 class flares) without saturating the detector and without the need for disruptive movable attenuators. These measurements will be used to: (1) investigate subsecond variations in HXR flux that strongly constrain flare acceleration timescales; (2) perform a

mission of opportunity by co-observing HXRs from solar flares along with the Spectrometer/Telescope for Imaging X-rays (STIX) onboard Solar Orbiter, systematically studying directivity; and serve as a HXR monitor of flares associated with solar eruptive events that will drive space weather in the next solar cycle. The IMPRESS concept of operations (CONOP) is shown in Figure 1 and consists of the following three key operations:

- Pointing the x-ray spectrometer at the Sun and collecting data.
- Transmitting the collected data to the ground using one of five transmitters located at different locations in the continental United States.
- Periodically charge the CubeSat's batteries by pointing solar panels at the sun.

Experiments in X-ray Characterization and Timing (EXACT) is another 3U CubeSat mission that will use an x-ray spectrometer similar to the one on IMPRESS. However, in the case of EXACT the x-ray spectrometer will be pointed at the pulsar in the Crab Nebula (PSR B0531+21). The detector will time-tag the times of arrival of x-ray photons from the pulsar that will be post-processed in support of developing algorithms for x-ray navigation (XNAV). Pulsar-based XNAV is a concept that is being explored for providing an autonomous means of positioning, navigation and timing (PNT) in deep space. Currently, the Deep Space Network (DSN) is used for these application. DNS is not an autonomous solution, but requires that the spacecraft seeking a PNT solution communicate with a triad of transmitters on Earth. By using x-ray pulsars as beacons generating a navigation signal, XNAV promises to provide an autonomous PNT solution in deep space. The data collected from EXACT and transmitted to Earth will be used to validate novel spacecraft ranging and timing algorithms.[2,3] It will also be used to develop algorithms for generating templates of pulsar signals using methods from machine learning. The CONOP for EXACT is very similar to that of IMPRESS, with the primary difference being the target at which the x-ray detector will be pointed.

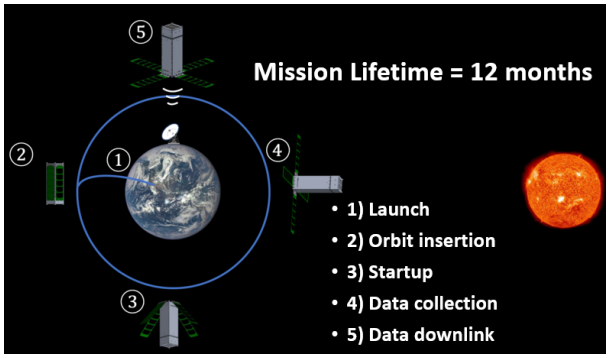

Figure 1: Concept of Operations (CONOPS) for the IMPRESS mission.

IMPRESS and EXACT are nearly identical CubeSat with the exception of minor differences in the design of their payload sensor. For attitude determination they use an algorithm that fuses measurements from a triad of rate gyros and magnetometers in an Extended Kalman Filter.[4] There are two options for attitude control systems: three-axis magnetometers and three-axis reaction wheels. For the sake of simplicity and cost, IMPRESS and EXACT are going to be built with three-axis magnetic torquers for attitude control. However, here we consider the case where reaction wheels are used for attitude control. While they have a larger bandwidth than magnetic torquers, three axis reaction wheels are power hungry. Thus, it would be interesting to see if it is possible to design a mission that maximizes science data returned without draining the battery and putting the CubeSats in a non-recoverable state. This approach also allows us to avoid the complexities of attitude control using magnetic torquers, which provide an instantaneously uncontrollable attitude system. This paper describes algorithms used for developing optimal mission plans for IMPRESS and EXACT under the assumption of reaction wheel control. In particular, it describes how to develop a schedule for the above mentioned operations described in Figure 1.

Prior Work

The problem of planning satellite maneuvers has received attention in the literature. The approaches range from high-level, abstracted approaches to granular, optimal control-based solutions. Recently, Li et al. have studied a planning problem for Earth-imaging satellites within the framework of formal methods and temporal logics.[5] While the attitude parameterization is simplified in this approach, the expressiveness of temporal logic lends itself to describing complex missions. Gabrel et al., Lemaitre

et al., She et al., and Cordeau et al. deal with Earth-imaging applications but apply a integer-based or graph-theoretic strategy.[6–9] Spangelo et al. take a similar approach but study the problem of ground station selection.[10] Approaches that leverage gradient methods for optimization include the work of Hwang et al., Qiu et al., and Wie et al.[11–13] These gradient methods scale very nicely, but are difficult to generalize across problems due to the nonconvexity of satellite attitude, which is unavoidable when designing global attitude guidance. In this work, we build on the existing integer-based methods in the literature by considering the impact of onboard systems on the feasibility of a given attitude guidance plan. This approach benefits from added fidelity and realism over strategies that do not consider the coupling between energy usage, data handling, and attitude guidance.

Problem Statement

In general, we would like to solve an optimization problem in which we choose actuator input trajectories that maximize the amount of scientific data we downlink from IMPRESS or EXACT, all the while ensuring the battery remain non-empty. This problem can be classified as a nonlinear optimal control problem. More specifically, this general problem is nonconvex and potentially nonsmooth (the nonconvexity arises from nonconvexity of attitude, and the nonsmoothness is an outcome of the modelling of data storage and battery level). Problems of this nature are very difficult to solve in general, so in this work we focus on a sub-problem; generating optimal attitude guidance for a CubeSat mission. In this formulation, rather than determine optimal actuator inputs for our mission, we determine optimal attitude *guidance* for the mission that a low-level controller can track.

Assume we wish to perform this optimization over a mission horizon of $[t_0, t_f]$. We discretize this timespan into timesteps $k \in \{0, ..., N\}$. Let $\mathcal{A}$ be a sequence of CubeSat attitudes in which an attitude is defined at each $k \in \{0, ..., N\}$. Let the amount of data transmitted to the ground by timestep k be $G(k)$, and the amount of energy stored in the battery be $E(k)$. Then, our optimal guidance problem is defined by Problem 1.

Problem 1

$$\begin{aligned} & \max_{\mathcal{A}} \quad G(N) \\ \text{subject to} \quad & E > E_{min} \\ & \text{dynamics} \end{aligned}$$

The remainder of this paper outlines our strategy for solving Problem 1.

Paper Organization

The remainder of this paper is organized as follows: The Methodology section details the modelling of onboard power consumption and data handling, attitude propagation, and the visibility of the targets of interest to each CubeSat (such as the Sun and ground stations). The Results section demonstrates the performance of our proposed method on case studies for EXACT and IMPRESS, and the Conclusions and Future Work section brings the paper to a close.

Methodology

Both IMPRESS and EXACT have missions with time-varying attitude requirements. That is, at some instances they may point at their primary science target (the Sun for IMPRESS and the Crab Nebula for EXACT), at other times they may point towards ground stations to transmit their collected data, and EXACT specifically will need to deliberately point at the Sun to collect power. Not only are there multiple attitude targets, but each of these targets is visible (to the spacecraft) only at specific times that depend on the CubeSat's orbit. This Section details the attitude, power, data handling, and visibility/occlusion modelling that contribute to the optimization procedure.

Reference Frames

Since we aim to optimally design a sequence of attitudes for IMPRESS and EXACT, it makes sense to define what we mean by attitude. There are many *parameterizations* of attitude, including Euler angles, quaternions, and direction cosine matrices (DCMs). We choose to work directly with the DCM here. Though both IMPRESS and EXACT have deployable solar panels, we model them as rigid bodies, meaning a single attitude describes the orientation of the entire spacecraft.

To model components and directions fixed to the CubeSat, we define a body frame which is rigidly fixed to the spacecraft. We define the body frame to align with the principal axes of inertia, making the inertia tensor diagonal when expressed in the body frame. Vectors in the body frame are denoted with subscript $\mathcal{B}$. We also define an Earth-centered, inertial (ECI) frame, denoted with subscript $\mathcal{I}$. This frame's 3-axis is aligned with Earth's rotational axis, its 1-axis points toward the vernal equinox, and its

2-axis completes the right-handed system. We denote the DCM which maps vectors in the ECI frame into the body frame by $\boldsymbol{C}_{\mathcal{BI}}$, and a vector in ECI $\boldsymbol{v}_{\mathcal{I}}$ can be expressed in the body frame by simple matrix multiplication:

$$\boldsymbol{v}_{\mathcal{B}} = \boldsymbol{C}_{\mathcal{BI}}\boldsymbol{v}_{\mathcal{I}}$$

To transform in the other direction, we can use the fact that the DCM is orthonormal: $\boldsymbol{C}_{\mathcal{BI}}^{-1} = \boldsymbol{C}_{\mathcal{BI}}^{\mathsf{T}}$ and define the map from body frame to ECI by reversing the subscripts:

$$\boldsymbol{C}_{\mathcal{IB}} = \boldsymbol{C}_{\mathcal{BI}}^{-1} = \boldsymbol{C}_{\mathcal{BI}}^{\mathsf{T}}. \tag{1}$$

In addition to the body and inertial frames, we also wish to track terrestrial targets such as ground stations. This motivates the use of another frame; the Earth-centered, Earth-fixed (ECEF). We denote vectors in this frame with subscript $\mathcal{F}$. Following the WGS84 standard, there is a DCM transforming vectors from ECI to ECEF which is a known function of time.[14] We represent this DCM by $\boldsymbol{C}_{\mathcal{FI}}(t)$.

Targets and Viewability

In order for an onboard system to view its distant target, we need a model for when target objects are visible from the spacecraft. For example, to assess if solar power is received by solar panels onboard, we must check that the panel normal direction points towards the Sun *and* that the Sun is not blocked by Earth. We refer to the question of whether the onboard system (like a solar panel) is oriented appropriately as a *viewing* problem, and the question of whether the Earth is blocking line of sight as an *occlusion* problem. This Section presents models for answering both questions.

We can assess whether a target object is blocked by Earth (from the perspective of a spacecraft) by considering the dot product of the spacecraft's position with the direction from the spacecraft to the target. More specifically, we can define bounds on that dot product, outside which the target is occluded by Earth, and inside which the target is visible to the spacecraft. However, this condition differs for distant targets in space (celestial targets) and targets on Earth's surface (terrestrial targets). For a celestial target located at position $\boldsymbol{q}_{\mathcal{I}}^{c}$ (expressed in the ECI frame), and for spacecraft located at $\boldsymbol{r}_{\mathcal{I}}$, let b_{qc}^{O} be a Boolean variable defined:

$$b_{qc}^{O} = \begin{cases} 1, & \frac{\boldsymbol{r}_{\mathcal{I}}^{\mathsf{T}}\boldsymbol{q}_{\mathcal{I}}^{c}}{\|\boldsymbol{r}_{\mathcal{I}}\|\|\boldsymbol{q}_{\mathcal{I}}^{c}\|} > -\sqrt{1 - R_E^2/\|\boldsymbol{r}_{\mathcal{I}}\|^2} \\ 0, & \text{otherwise} \end{cases} \tag{2}$$

where R_E is Earth's mean radius. For any celestial target, we can define $\boldsymbol{q}_{\mathcal{I}}^{c}$ and a plane perpendicular to that vector. Equation 2 checks that the projection of the satellite's position into that plane has length greater than Earth's radius and returns 1 if a line-of-sight exists between the satellite and the target.

We can carry out a similar analysis for terrestrial targets with an additional consideration: An elevation mask is included to model tree cover or buildings surrounding the target. Standing at a target location on Earth, the elevation mask is the angle above the horizon the satellite must make in order to contact the target. However, we work with the cone angle defined by the elevation mask which is simply 90° minus the mask angle. This cone has an axis which is the position vector of the target, and its half-angle is denoted α_g. Then, if a terrestrial target has position $\boldsymbol{q}_{\mathcal{I}}^{g}$, let b_{qg}^{O} be a Boolean variable defined:

$$b_{qg}^{O} = \begin{cases} 1, & \frac{(\boldsymbol{r}_{\mathcal{I}} - \boldsymbol{q}_{\mathcal{I}}^{g})^{\mathsf{T}}\boldsymbol{q}_{\mathcal{I}}^{g}}{\|\boldsymbol{r}_{\mathcal{I}} - \boldsymbol{q}_{\mathcal{I}}^{g}\|\|\boldsymbol{q}_{\mathcal{I}}^{g}\|} > \alpha_g \\ 0, & \text{otherwise} \end{cases} \tag{3}$$

Note that objects on Earth's surface such as ground stations are typically located with latitude and longitude coordinates. Conveniently, these can be easily converted to ECEF coordinates using the WGS84 standard, and from there converted to ECI.[14] This allows us to determine $\boldsymbol{q}_{\mathcal{I}}^{g}$ given the target's latitude and longitude, and time.

Even if b_{qc}^{O} or b_{qg}^{O} is true for some target, in order to establish "contact" with the target (receive power or stream data) the satellite must have the appropriate attitude. To model this, we introduce two more Boolean variables; b_{qc}^{V} for celestial targets and b_{qg}^{V} for terrestrial targets. Let $\boldsymbol{q}_{\mathcal{B}^*}^{c}$ represent the vector in the body frame we wish to point at target $\boldsymbol{q}_{\mathcal{I}}^{c}$ (such as a solar panel normal at the Sun), and $\boldsymbol{q}_{\mathcal{B}^*}^{g}$ represent the vector in the body frame we wish to point at target $\boldsymbol{q}_{\mathcal{I}}^{g}$ (such as an antenna at a ground station). Additionally, we assume all onboard sensors have conic constraints on their pointing—in order to collect data from the Crab Nebula for example, EXACT must point its detector with a certain angular distance from the Crab Nebula. Outside of this cone, we assume no data is received. For a celestial target $\boldsymbol{q}_{\mathcal{I}}^{c}$, denote the corresponding cone half-angle by γ_q^c, and for terrestrial target $\boldsymbol{q}_{\mathcal{I}}^{g}$, denote the corresponding cone half-angle by γ_q^g. Then,

$$b_{qc}^{V} = \begin{cases} 1, & \frac{\boldsymbol{q}_{\mathcal{B}^*}^{c\mathsf{T}}\boldsymbol{C}_{\mathcal{BI}}\boldsymbol{q}_{\mathcal{I}}^{c}}{\|\boldsymbol{q}_{\mathcal{B}^*}^{c}\|\|\boldsymbol{q}_{\mathcal{I}}^{c}\|} > \cos\gamma_q^c \\ 0, & \text{otherwise} \end{cases} \tag{4}$$

and

$$b_{qg}^V = \begin{cases} 1, & \frac{\boldsymbol{q}_{\mathcal{B}^*}^{g^\mathsf{T}} \boldsymbol{C}_{\mathcal{BI}} (\boldsymbol{r}_\mathcal{I} - \boldsymbol{q}_\mathcal{I}^g)}{\|\boldsymbol{q}_{\mathcal{B}^*}^g\| \|\boldsymbol{r}_\mathcal{I} - \boldsymbol{q}_\mathcal{I}^g\|} > \cos\gamma_q^g \\ 0, & \text{otherwise} \end{cases} \tag{5}$$

Like with their occlusion-checking counterparts, b_{qc}^V and b_{qg}^V are true when the satellite's attitude points the appropriate onboard sensor at the target. Note that in order to receive power, for example, *both* b_{qc}^O and b_{qc}^V for the Sun must be true, and in general the pair of Boolean variables may be true independently of one another.

While this exposition of occlusion and viewing conditions has used the symbol q for a generic vector, for the application area of this paper we define three main targets: the Sun, the science target, and ground stations. We also drop the subscript or superscript c or g denoting a celestial or terrestrial target as it is evident from context. Variables related to the Sun are represented by symbol s: the Sun's position is $\boldsymbol{s}_\mathcal{I}$, the solar panel normal direction is $\boldsymbol{s}_{\mathcal{B}^*}$, the Boolean variable for solar occlusion is b_s^O, and the Boolean variable for solar viewing is s_s^V. Likewise, variables related to the science target are represented by d: the science target's position is $\boldsymbol{d}_\mathcal{I}$, the onboard science instrument's boresight axis is $\boldsymbol{d}_{\mathcal{B}^*}$, the Boolean variable for science target occlusion is b_d^O, and the Boolean variable for science target is b_d^V. Finally, because there are multiple ground stations, they are indexed by a superscript l and are represented by g^l: the lth ground station's position is $\boldsymbol{g}_\mathcal{I}^l$, the antenna's normal direction is $\boldsymbol{g}_{\mathcal{B}^*}$, the Boolean variable for ground station occlusion is b_{gl}^O, and the Boolean variable for ground station viewing is b_{gl}^V.

Node Definition

As defined earlier, Problem 1 is ambiguous because the set of feasible attitude trajectories $\mathcal{A}$ has not yet been defined. There are two constituents of $\mathcal{A}$ to resolve. The first is the discrete time steps at which we will choose attitude. The second is the set of allowable attitudes at those steps. To determine times at which to make maneuvers, we first track the positions of the satellite and its targets (Sun, ground stations, and Crab Nebula for EXACT) over time. Then, using the definitions in the previous section, we determine time windows for each target in which the target is unoccluded by Earth from the satellite's perspective. Given these time windows, we examine the start and endpoints of the windows and make the following three assumptions about our attitude guidance:

1. If a target *becomes* visible at a timestep, we may want to point at it.

2. If a target *ceases to be* visible at a timestep but other targets remain visible, we may want to choose one of those other targets to point at.

3. Assume attitude remains unchanged between maneuvers.

So in summary, we will assume attitude is constant unless we choose a new attitude at a node, where nodes exist either where a target becomes visible, or ceases to be visible while other targets remain visible. Once we have defined nodes for the mission, we optimize by finding a path joining nodes that results in maximum data downlink without draining the battery.

State Propagation

Because our optimization strategy involves propagating attitude, battery level, and data transmitted to Earth between nodes, we define the discrete-time dynamics of these quantities here. In addition to onboard battery level E and downlinked data volume G, we also track the onboard data stored with variable S. These quantities are propagated over the time difference between two nodes, Δt as follows:

$$E(k+1) = E(k) + \Big(P^{in}(k) - P^{out}(k)\Big)\Delta t \tag{6}$$

$$S(k+1) = S(k) + \Big(D^{in}(k) - D^{out}(k)\Big)\Delta t \tag{7}$$

$$G(k+1) = G(k) + D^{out}(k)\Delta t \tag{8}$$

where P^{in} and P^{out} are respectively the power input and output from the satellite, and D^{in} and D^{out} are respectively the data rates in and out of the satellite.

The power generated by solar panels P^{in} depends on the vector to the Sun $\boldsymbol{s}_\mathcal{I}$, and the solar panel normal vector $\boldsymbol{s}_{\mathcal{B}^*}$:

$$P^{in} = b_s^O b_s^V G_0 A \eta \frac{\boldsymbol{s}_{\mathcal{B}^*}^\mathsf{T} \boldsymbol{C}_{\mathcal{BI}} \boldsymbol{s}_\mathcal{I}}{\|\boldsymbol{s}_{\mathcal{B}^*}\| \, \|\boldsymbol{s}_\mathcal{I}\|} \tag{9}$$

where $G_0 = 1361$ W/m^2 is the solar irradiance constant at 1 AU, A is the solar panel area, and η is solar panel efficiency. The fractional term is equal to the cosine of the angle between solar panel normal and Sun direction vectors. The power output has three components: A constant background power consumption, power required to run the science instrument P^d, and power required to transmit over

radio P^g:

$$P^{out} = \overline{P}^{out} + b_d^V b_d^O P^d + b_{gl}^V b_{gl}^O P^g \tag{10}$$

The data input to the onboard storage is simply:

$$D^{in} = \overline{D}^{in} + b_d^V b_d^O D^d \tag{11}$$

where $\overline{D}^{in}$ is a constant background data rate to account for the generation of housekeeping data, and D^d is the data rate from the science instrument when it is active. Similarly, the output data rate is:

$$D^{out} = b_{gl}^V b_{gl}^O D^g \tag{12}$$

where D^g is a constant downlink data rate to the ground station. Equations 6-12 define rules to propagate battery level, onboard data storage, and ground station data between nodes in our discrete framework. What remains is a method to propagate attitude.

Before defining the method for attitude propagation, consider an illustrative example: Assume we have chosen to point an antenna at the ground station. Once we have aligned the antenna vector with the vector pointing to the ground station, we can rotate the satellite freely about that vector. Our strategy for propagating attitude must be able to resolve this leftover degree of freedom to be deterministic. To handle this, we leverage the axis-angle parameterization of attitude. This parameterization is based on a theorem due to Euler; that any change in attitude can be decomposed into a rotation by some angle about a fixed axis. Let that axis be $\boldsymbol{a}_{\mathcal{BI}}$, and the angle $\phi_{\mathcal{BI}}$. Then, we can extract a DCM from this parameterization as follows:

$$\begin{aligned}\boldsymbol{C}_{\mathcal{BI}} = \mathbf{1}\cos\phi_{\mathcal{BI}} + (1-\cos\phi_{\mathcal{BI}})\boldsymbol{a}_{\mathcal{BI}}\boldsymbol{a}_{\mathcal{BI}}^{\mathsf{T}} + \\ + \boldsymbol{a}_{\mathcal{BI}}^{\times}\sin\phi_{\mathcal{BI}}\end{aligned} \tag{13}$$

where $\mathbf{1}$ is the 3×3 identity matrix, and $(\cdot)^{\times}: \mathbb{R}^3 \to \mathfrak{so}(3)$ is the skew-symmetric operator. Given a target object's position $\boldsymbol{q}_{\mathcal{I}}$ and its corresponding body vector $\boldsymbol{q}_{\mathcal{B}^*}$, we can find the axis and angle with the following:

$$\boldsymbol{a}_{\mathcal{BI}} = \frac{\boldsymbol{q}_{\mathcal{I}}^{\times}\boldsymbol{q}_{\mathcal{B}^*}}{\left\|\boldsymbol{q}_{\mathcal{I}}^{\times}\boldsymbol{q}_{\mathcal{B}^*}\right\|} \tag{14}$$

$$\phi_{\mathcal{BI}} = \cos^{-1}\left(\frac{\boldsymbol{q}_{\mathcal{I}}^{\mathsf{T}}\boldsymbol{q}_{\mathcal{B}^*}}{\left\|\boldsymbol{q}_{\mathcal{I}}^{\mathsf{T}}\boldsymbol{q}_{\mathcal{B}^*}\right\|}\right) \tag{15}$$

Using the above expressions at any node, we can uniquely define attitude for any given target.

Optimization Strategy

We interpret the nodes defined previously to form a directed acyclic graph, in which we can choose to move from a starting node (defining initial attitude, battery level, and onboard storage) to any node in the future. The structure of this graph is simple: each node has an edge connecting to each node in the future. Thus, our optimization procedure is to find the path through this graph that generates the most data on the ground by the end, yet does not drain the battery. This optimization problem falls in the class of integer programs, as it deals with best choice of discrete attitudes at discrete times. Though shortest/longest path algorithms are capable at solving the integer problem for a variety of graph topologies[15–17] our problem cannot be solved by these standard methods because the cost is path dependent. Because the battery level at the current node depends on the nodes visited previously (and the power received and spent there), we do not know *a priori* the cost of traversing each edge in the graph. This results in a combinatorial optimization problem, i.e. every path's cost must be assessed to find the optimum. Problems of this nature are formidable to solve as they scale terribly. In the case of our attitude guidance problem, an increase in number of targets or length of time horizon will result in an exponential increase in the number of paths to check.

Fortunately, there are some strategies we adopt to expedite the optimization. First, given the set of nodes (which is known *a priori*), we can enumerate all paths efficiently using a Depth-First Search (DFS) algorithm. While it is costly to propagate attitude, battery level, and data stored onboard between nodes, it is computationally inexpensive to check the target object associated with a given node. This provides two avenues along which to speed up our optimization: pruning and prioritization. First, based on the battery capacities of IMPRESS and EXACT (and many CubeSats), it is unwise to go several orbits without ever pointing solar panels at the Sun. So, we immediately prune out paths which do not visit the Sun once per orbit. Then, considering the objectives of IMPRESS and EXACT to transmit as much scientific data to the ground as possible (an objective generalizable to many other scientific CubeSat missions), we count all the ground station nodes per path, then order all the paths in decreasing count of ground station nodes. Because we aim to downlink as much data as possible, it makes sense to first search paths with many ground station passes before searching paths with

few ground station passes. (IMPRESS and EXACT will be in circular orbits, and all of the ground stations have similar elevation masks, so every node corresponding to a ground station will admit roughly the same amount of data transmission). If a feasible solution is found (one that does not empty the battery), then we terminate the optimization after all paths with the same number of ground stations have been searched.

Results

To demonstrate the proposed optimal attitude guidance strategy, we present results of the method applied to the same two-orbit scenario for both IMPRESS and EXACT. Both satellites share a common bus, so their geometric, electrical, and data handling properties are identical and tabulated in Table 1. They differ in their mission target—IMPRESS points its detector at the Sun, and EXACT points at the Crab Nebula. These two targets also produce different amounts of data onboard due to their different fluxes: the Crab Nebula generates about 1.53 kbps when viewed by EXACT, whereas the Sun generates about 35.9 kbps when viewed by IMPRESS.[18] Both satellites have access to an array of five ground stations managed by the Aerospace Corporation. We assume here that IMPRESS and EXACT can communicate freely with any of these ground stations at any time. Simulations were run on a laptop with a 3.1 GHz Intel processor and 8 GB RAM, and terminated in under two minutes for the scenarios shown here.

Table 1: EXACT and IMPRESS Parameters

Variable	Symbol	Value	Units
Inertia tensor	$\boldsymbol{I}_{\mathcal{B}}$	$\text{diag}(0.25, 0.25, 0.5) \times 10^{-4}$	kg m^2
Minimum battery level	E_{min}	30	W hr
Maximum battery level	E_{max}	40	W hr
Solar irradiance constant	G_0	1361	W/m^2
Solar panel area	A	0.12	m^2
Solar panel efficiency	η	0.29	—
Solar panel normal direction	$\boldsymbol{s}_{\mathcal{B}^*}$	$\begin{bmatrix}0 & 0 & 1\end{bmatrix}^\mathsf{T}$	—
Detector boresight direction	$\boldsymbol{d}_{\mathcal{B}^*}$	$\begin{bmatrix}0 & 0 & 1\end{bmatrix}^\mathsf{T}$	—
Antenna direction	$\boldsymbol{g}_{\mathcal{B}^*}$	$\begin{bmatrix}0 & 0 & -1\end{bmatrix}^\mathsf{T}$	—
Baseline output power	$\overline{P}^{out}$	9	W
Detector power consumption	P^d	10.5	W
Radio power consumption	P^g	4.5	W
Baseline input data rate	$\overline{D}^{in}$	4	kb/s
EXACT input data rate from Crab nebula	D^d	1.53	kb/s
IMPRESS input data rate from Sun	D^d	35.9	kb/s
Output data rate	D^g	500	kb/s
Groundstation cone half-angle	α_g	40	deg
Radio antenna cone half-angle	γ_g	30	deg
Detector cone half-angle	γ_g	45	deg

Case Studies

Orbits for both CubeSats were propagated using Newtonian gravity plus a J2 perturbation. Then, the occlusion analysis outlined in the previous Section was performed to determine windows of availability for each target. Windows of availability for each target are shown in Figure 2.

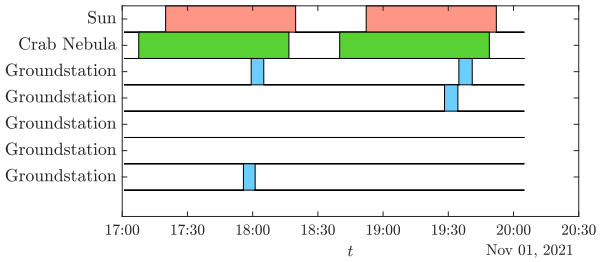

Figure 2: Occlusion of targets.

The time spans in which the Sun is not occluded by Earth (day time) are shown in red, the spans in which the Crab Nebula is visible are shown in green, and the ground station windows are shown in blue. Based on these windows, nodes at which to select a new attitude where identified. The nodes were connected in a graph, which is shown in Figure 3.

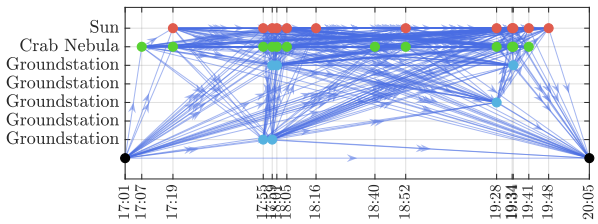

Figure 3: Graph with nodes and attitude transition opportunities.

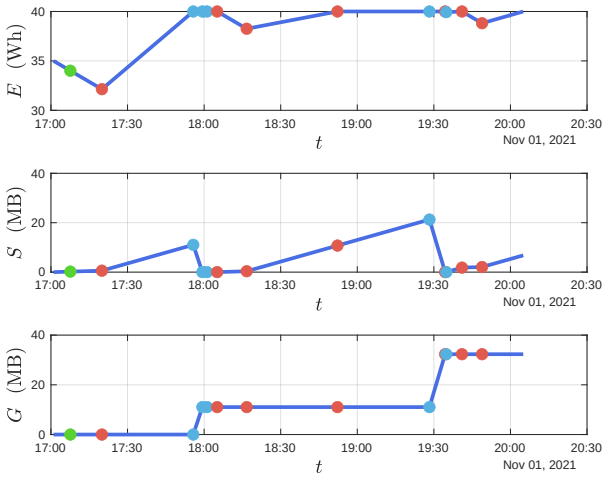

Figure 4: State history for IMPRESS.

Like in Figure 2, nodes are color-coded by their target, with red nodes for the Sun, green for the Crab nebula, and light blue for ground stations. Additionally, the intial and final black nodes are added to ensure neutral initial and terminal conditions. This graph then was pruned and ordered using a depth-first search enumeration of its paths. For each feasible path, onboard battery level, data volume stored, and data volume downlinked to ground stations were propagated along the path. Finally, the feasible solution with maximum downlinked data was selected as the optimum.

The optimal node sequence for IMPRESS is shown in Figure 4. The lines in each plot show the history of each state variable (E, S, G), and the colored dots indicate the target chosen at each time. Note that for IMPRESS, green corresponds to the Sun, not the Crab Nebula. Because the scenario is initialized with 50% battery, the optimizer selects the Sun as the target as soon as it becomes available. Conveniently, this target is also the science target for IMPRESS, so a simultaneous increase in onboard power is observed. Later (around 18:00) when the first ground station comes into view, it is selected and all onboard data is offloaded in one pass (note that the downlinking data rate is much higher than the rate at which science data is received). Next, IMPRESS again is directed to point at the Sun, accumulating additional data onboard until the next ground station pass where it offloads its accumulated data, totalling approximately 33 MB of science and housekeeping data transmitted.

The optimized state history for EXACT is shown in Figure 5. Like the IMPRESS plots, the lines represent state histories and the colored dots indicate the target chosen. Like IMPRESS, the optimizer chooses to point at the Sun as soon as it becomes available to avoid emptying the battery. Unlike IMPRESS, however, EXACT's science data rate is very low, and the increase in S from the beginning of the simulation is attributable to the accumulation of housekeeping data alone. When the first ground station becomes available, the accumulated housekeeping data is downlinked before EXACT returns to Sun pointing. Around 18:40 there is a notable excursion to point at the Crab nebula (in green), but this does not produce a visible change in data accumulated—this is because the science data rate and housekeeping data rate are of similar magnitude for EXACT. The optimizer then switches back to Sun-pointing before downlinking at the next ground station pass. Finally, as with IMPRESS, there are a few maneuvers after the last groundstation pass. However, these are effectively slack in the optimizer as they cannot affect the data transmitted to the ground.

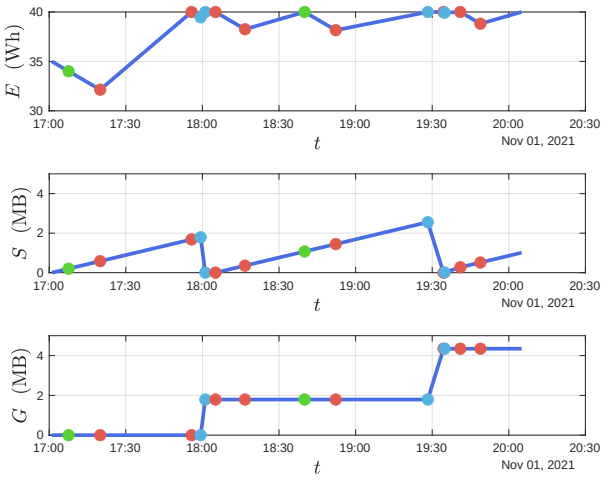

Figure 5: State history for EXACT.

The optimizer's lack of interest in the true science target of the EXACT mission is of concern. Though it makes sense given the optimization strategy, it violates the intuition that science data from a CubeSat is worth more to the analyst on the ground than housekeeping data. Despite this shortcoming, the proposed method seems to perform well for scenarious presented here. In both cases, the time to build the graph and solve was under two minutes, far faster than real-time and suitable for planning maneuvers for CubeSats in orbit.

Conclusions and Future Work

The proposed approach has been demonstrated to work well for the IMPRESS and EXACT missions. In the case studies shown, the proposed optimization strategy successfully maintained battery level above empty while maximizing the data transmitted to the ground over the mission. Furthermore, the method runs faster than real time on a laptop for small numbers of orbits—an encouraging sign for the practicality of this approach. The search strategy is also trivially parallelizable for larger problems, indicating potential avenues to expand the optimization horizon and problem complexity.

However, this strategy does have notable shortcomings. The fact that the formulation is a combinatorial integer problem ensures it will scale poorly—regardless of parallel processing or other improved computational resources, solution time will grow exponentially with the complexity of the problem. Reformulating Problem 1 as a differentiable problem would enable the use of gradient-based optimizers which scale very well compared to integer methods. Another limitation of our approach is in neglecting attitude perturbations. In reality, attitude perturbations such as the gravity gradient moment, magnetic torques, and differential atmospheric drag will contribute non-negligibly to the cost of a maneuver and should be accounted for in a more holistic optimization environment. Finally, the optimizer's ignorance of the difference between housekeeping and primary science data will need to be addressed in future work to make this method an attractive solution to mission-aware attitude guidance problems for CubeSats.

Acknowledgement

The authors would like to thank the National Science Foundation for supporting this project. This paper is based upon work supported by the National Science Foundation under Grant No. 1841006, and by the United States Airforce though the University Nanosat Program (UNP). Any opinions, findings, and conclusions or recommendations expressed in this material are those of the authors and do not necessarily reflect the views of the National Science Foundation or the United States Airforce.

References

[1] Lindsay Glesener, Demoz Gebre-Egziabher, John Sample, Amir Caspi, and et. al. The IMpulsive Phase Rapid Energetic Solar Spectrometer (IMPRESS) . In *Proceedings of the SPIE Photonics and Optics Conference*. SPIE, 2021.

[2] Joel Runnels and Demoz Gebre-Egziabher. Recursive Range Estimation Using Astrophysical Signals of Opportunity. *AIAA Journal of Guidance, Control and Dynamics*, 6(40), 2017.

[3] Joel Runnels. *Six Degree of Freedom Navigation Using X-Ray Pulsar Signals*. PhD dissertation, University of Minnesota, Twin Cities Campus, 2019.

[4] Kail Laughlin. *Single-Vector Aiding of an IMU for CubeSat Attitude Determination*. Masters thesis, University of Minnesota, Twin Cities Campus, 2020.

[5] Jianqing Li, Chaoyong Li, and Feng Wang. Automatic Scheduling for Earth Observation Satellite With Temporal Specifications. *IEEE Transactions on Aerospace and Electronic Systems*, 56(4):3162–3169, 2020.

[6] Virginie Gabrel and Daniel Vanderpooten. Enumeration and interactive selection of efficient paths in a multiple criteria graph for scheduling

an earth observing satellite. *European Journal of Operational Research*, 139:533–542, 2002.

[7] Michel Lemaître, Gérard Verfaillie, Frank Jouhaud, Jean-michel Lachiver, and Nicolas Bataille. Selecting and scheduling observations of agile satellites. *Aerospace Science and Technology*, 6:367–381, 2002.

[8] Yuchen She, Shuang Li, and Yanbin Zhao. Onboard mission planning for agile satellite using modified mixed-integer linear programming. *Aerospace Science and Technology*, 72:204–216, 2018.

[9] J. F. Cordeau and G. Laporte. Maximizing the value of an earth observation satellite orbit. *Journal of the Operational Research Society*, 56(8):962–968, 2005.

[10] Sara Spangelo, James Cutler, Kyle Gilson, and Amy Cohn. Computers & Operations Research Optimization-based scheduling for the single-satellite , multi-ground station communication problem. *Computers and Operation Research*, 57:1–16, 2015.

[11] John T Hwang, Dae Young Lee, James W Cutler, and Joaquim R R A Martins. Large-Scale Multidisciplinary Optimization of a Small Satellite ' s Design and Operation. *AIAA Journal of Spacecraft and Rockets*, 51(5), 2014.

[12] Wei Qiu and Chao Xu. Attitude Maneuver Planning of Agile Satellites for Time Delay Integration Imaging. *Journal of Guideance, Control, and Dynamics*, 43(1):46–59, 2020.

[13] Bong Wie, David Bailey, and Christopher Heiberg. Rapid multitarget acquisition and pointing control of agile spacecraft. *Journal of Guidance, Control, and Dynamics*, 25(1):96–104, 2002.

[14] Department of Defense World Geodetic System 1984: Its Definition and Relationships with Local Geodetic Systems. Technical report, 1991.

[15] Edsger W. Dijkstra. A Note on Two Problems in Connection with Graphs. *Numerische Mathematik*, 1:269–271, 1959.

[16] Richard Bellman. On a routing problem. *Quarterly of Applied Mathematics*, 16:87–90, 1958.

[17] James J Kuffner and Steven M LaValle. RRT-Connect: An Efficient Approach to Single-Query Path Planning. *IEEE Transactions on Robotics and Automation*, 2000.

[18] Trevor Knuth. *Studying Particle Acceleration in Solar Flares via Subsecond X-ray Spikes: Analysis and Instrumentation.* PhD dissertation, University of Minnesota, Twin Cities Campus, 2021.